Adaptive WDMA: improving the data rate of a densely deployed LiFi network

Giovanni Luca Martena
University of Strathclyde
Glasgow, United Kingdom
giovanni.martena@strath.ac.uk

Rui Bian
pureLiFi Ltd.
Edinburgh, United Kingdom
rui.bian@purelifi.com

Harald Haas
University of Strathclyde
Glasgow, United Kingdom
harald.haas@strath.ac.uk

ABSTRACT

A novel adaptive Wavelength Division Multiple Access (WDMA) scheme is presented in this paper, capable of contrasting the effect of the Passband Shift (PS) phenomenon in an indoor densely deployed LiFi network. After an overview on WDMA in an indoor Internet of Things (IoT) setting, simulation work is defined and carried out. Results show how in such settings, the loss of connection is reduced to an average of 0.72 % compared to 31.25 % when using Adaptive WDMA. Additionally, the users are served with higher average speeds and better fairness.

CCS CONCEPTS

• **Networks** → **Network resources allocation**; *Network layer protocols*; • **Human-centered computing** → Ubiquitous and mobile devices.

KEYWORDS

lifi, wavelength division multiple access, owc, iot

ACM Reference Format:
Giovanni Luca Martena, Rui Bian, and Harald Haas. 2021. Adaptive WDMA: improving the data rate of a densely deployed LiFi network. In *Internet of Lights (IoL'21), June 25, 2021, Virtual, WI, USA.* ACM, New York, NY, USA, 6 pages. https://doi.org/10.1145/3469264.3469806

1 INTRODUCTION

Optical Wireless Communication (OWC) is drawing both academic and industrial interest due to the free, vast and unregulated spectrum it is able to provide. Moreover, the IoT and its wide applications seemingly form a good match with OWC [13] because of its speed, inherent security and lack of cables that would be a hindrance in massive deployments. The fact that OWC includes the use of visible light opens a range of possibilities in which a grid of lighting fixtures, acting as Access Points (APs), can deliver both communication and illumination functionalities. Such a fully-networked OWC system is termed LiFi [10], and is seen as an enabler for the IoT [6]. However this comes with a number of challenges, two of which consist of the random position and orientation that the users can take, along with their dense deployment. In fact, random position and orientation of users can significantly lower the power of the received signal, while increased User Equipment (UE) and AP density can strongly favour interference. The random orientation of users has been analysed in a number of studies ([1], [3], [4], [5]), which describe the associated challenges as well as providing various insights and potential solutions to cope with this issue. Other studies ([7], [8], [9]) consider the problem of random orientation from the wavelength division paradigm perspective, with [7] offering a solution to optimise the design of the optical filters' characteristics. This is an efficient way to mitigate the impact of the Passband Shift (PS) phenomenon. It consists of an inherent shift in the transmission characteristics of optical filters (passband edges and central wavelength) with the varying Angle of Incidence (AoI) of the impinging light. However, it should be noted that such an approach is heavily dependent on the front-end design. This can adversely impact the system's adaptability to the wide spectrum of different devices that IoT includes. In fact, these range from smartphones, smartwatches and laptop computers, to various home appliances and industrial machinery pertaining to the concepts of Smart Home and Industry 4.0. The goal of this paper is to propose a Wavelength Division Multiple Access (WDMA) scheme suitable for low-complexity and high-mobility devices, which is able to contrast the combined effects of the PS phenomenon and the random orientation of devices in an everyday use case. The rest of this paper is organised as follows: in Section 2, the context and challenges associated with WDMA, along with the differences between Classic and Adaptive WDMA schemes, are explained. In Section 3, the channel model and Simulation characteristics are presented. In Section 4, the results of the simulations are presented and discussed. In Section 5, conclusions are drawn.

2 CONTEXT AND CHALLENGES

2.1 Wavelength Division Multiple Access

This work considers indoor IoT in dense deployments. The consequences of this are twofold: on one hand, there will be several kinds of UEs, whose complexity and mobility needs can range from low to high. Therefore, it is imperative to consider a constraint in terms of versatility. On the other hand, one can expect to have a high number of UEs competing for connection resources. It is intuitive to realise that as both UEs and APs increase in number, the interference increases proportionally, and is bound to become a major limitation for the system. This accounts for the main challenge that this work tackles, which is interference mitigation.

To achieve this, it is important to consider channel separation. In fact, properly separated channels will not interfere with one another, making it possible to deliver a better signal with less energy. WDMA offers channel separation by exploiting wavelength selectivity. For this reason, a WDMA-enabled AP consists of up to four coloured LEDs (typically Red, Green, Blue and Amber) while the corresponding receiver has up to four colour-filtered elements. Therefore, each UE will only have one of these elements active

IoL'21, June 25, 2021, Virtual, WI, USA

at any given time, based on the colour it has been assigned to. In this paper, a single coloured LED of a single AP will be referred to as a Transmitter Element (TE), while one single colour-filtered element at receiver side will be referred to as Receiver Element (RE). The difference between state-of-the-art WDMA, henceforth referred to as "Classic WDMA", and Adaptive WDMA, lies in how the channel assignment is managed. Classic WDMA employs a fixed allocation, where every user is assigned to a colour matching the TE-RE combination in a round-robin fashion. Thus, if 4 users enter the network at subsequent times, the assignation will happen in such a way that user 1 will receive the signal from the Blue TE with the Blue RE, user 2 will receive the signal from the Green TE with the Green RE, and so on.

Adaptive WDMA (described in detail in section 2.3) employs a dynamic allocation, in which every user is assigned a TE-RE combination without the necessity of colour matching. This guarantees a higher number of options when forming a channel, and enables the system to redistribute the available resources according to the actual orientation of the UEs. The added flexibility allows the unwanted effects of the PS phenomenon to be avoided, by using a RE whose spectral shift makes it more favourable to collect the signal at that particular orientation.

This process makes use of Channel State Information (CSI) to estimate the Signal-to-Interference-plus-Noise Ratio (SINR) of all possible TE-RE combinations, and then selects the one that maximises the aggregate SINR. The key aspect of this solution is that it effectively exploits the users' separation in terms of orientation to offer improved channel separation. Having more combinations that require SINR estimation, Adaptive WDMA comes at the cost of increased overheads. However, it should also be noted that it does not introduce a higher complexity for the UEs as the process can be implemented at a higher level. Moreover, this solution is not related to the specific front-end design, and while improvements on this aspect can certainly yield better performances, the choice of LEDs and optical filters does not directly impact its effectiveness.

Finally, it has to be noted that WDMA contemplates the use of individually addressable transmitters emitting at different wavelengths. This allows for the use of colour mixing schemes to provide smart lighting features. In an indoor IoT setting this is an advantage, as readings from different sensors can be used by the system to gather information on user behaviour and adjust the lighting settings according to the tasks that are to be carried out in a specific area.

2.2 The problem of Passband Shift

2.2.1 Random Orientation. As previously stated, it is crucial in a LiFi indoor IoT setting to account for the complexity and mobility needs of the devices that populate the environment. In terms of mobility, it is clear that the biggest challenge is posed by highly portable UEs such as smartphones and wearables. The impact of mobility and random orientation in OWC and LiFi has recently drawn rising attention, and has been studied in [3] - [12]. In [12], measurements have been carried out to gain insight on the orientation in space for such devices both in walking and sitting activities, in terms of azimuth and elevation angles. Results show that for walking activities, the azimuth angle can be represented with a uniform distribution ranging from 0° to 360°, while the elevation angle approaches a Gaussian distribution, with a mean of 30° and a standard deviation of less than 9°.

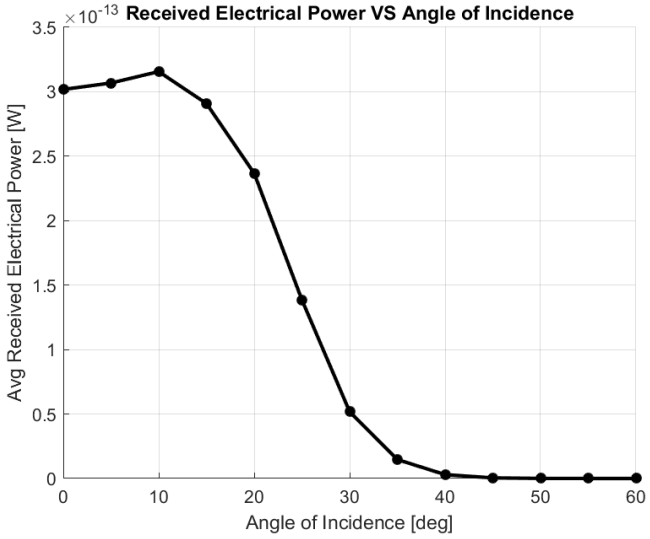

Figure 1: Average received electrical power vs angle of incidence. The received electrical power is averaged over four RGBA LEDs transmitting to four RGBA-filtered receivers. Due to the PS phenomenon, said power decreases substantially while increasing the AoI.

2.2.2 Passband Shift. The PS phenomenon for thin-film optical filters has been described in detail in [2]. It consists of a shift towards shorter wavelengths of the relative transmission spectra of such optical filters, with a dependence on the AoI of the impinging light. The shifted wavelength of an optical filter characteristic, $\lambda_{\mathrm{OF}}(\psi)$, dependent from the AoI, is then given as:

$$\lambda_{\mathrm{OF}}(\psi) = \lambda_{\mathrm{OF},\psi=0}\sqrt{1-\frac{\sin^2(\psi)}{n_{\mathrm{e}}^2}} \tag{1}$$

Where $\lambda_{\mathrm{OF},\psi=0}$ is the non-shifted wavelength of the considered transmission characteristic (namely, passband edges and central wavelength), ψ is the AoI of the impinging light, and n_{e} is the effective refractive index of the specific optical filter employed. It can be seen that for the values that ψ will likely take in an everyday use case, as described in sub-section 2.2.1, this phenomenon can become another important limitation to the channel separation capabilities of WDMA.

Figure 1 shows how this phenomenon can impact the performances of the system. It should be noted that the shape of the curve is heavily dependent on the front-end design, and more specifically on how well the LEDs' emission spectra and the optical filters' transmission spectra overlap. This figure is obtained with the same LEDs and optical filters used throughout the rest of the paper. As it can be seen, the received electrical power decays substantially with relatively small modifications to the AoI.

2.3 Adaptive WDMA Algorithm

In this section, the Adaptive WDMA Algorithm is explained in detail. As previously stated, it aims to maximise the aggregate SINR over all UEs. This is achieved by increasing the number of TE-RE combinations available to each user to up to 7, and by selecting the best combination to serve each user. These combinations are:

- Blue TE and Blue RE
- Blue TE and Green RE
- Green TE and Green RE
- Green TE and Amber RE
- Amber TE and Amber RE
- Amber TE and Red RE
- Red TE and Red RE

These take into account that, with the contribution of the PS phenomenon, certain user orientations could make it difficult to collect the signal with the RE and the same colour TE, and thus allow for increased flexibility. The algorithm requires that CSI is collected, and therefore it will be assumed that such information is available for the network. This knowledge makes it possible, even if two or more users are under the same AP, to compute the aggregate SINRs from which the highest will be selected. When dealing with the case of two or more users under the same AP, this computation encompasses two aspects: on one hand, it is necessary to evaluate the possible TE-UE assignations (e.g. Amber TE-UE 1 and Green TE-UE 2 VS Amber TE-UE 2 and Green TE-UE 1). On the other hand, for every TE-UE combination, there is the need to evaluate it if the signal has to be collected with the matching or non-matching RE. It should be noted that these computations can be carried out at the network level, and therefore will also be suitable for low-complexity UEs. This algorithm can be detailed as follows:

for $UE = 1, 2, \ldots$ **do**
  Assign Central AP to UE based on highest Signal Strength;
end
for $AP = 1, 2, \ldots$ **do**
  if *AP is Central for exactly 1 UE* **then**
    Compute SINR for each TE-RE combination;
    Assign that UE to the TE-RE combination that maximises SINR;
  end
  if *AP is Central for 2 or more UEs* **then**
    Compute aggregate SINR for each TE-UE-RE combination;
    Assign UEs to TE-RE combinations that maximise aggregate SINR;
  end
end

Algorithm 1: Adaptive WDMA

3 CHANNEL AND SIMULATIONS

3.1 Channel Model

As it is common in the field of OWC, it is possible to employ a line of sight channel model, and use the channel DC gain to describe the optical power loss from the moment the light beam leaves the transmitter surface, until it hits the receiver. This is well described in literature (such as [11]), and it is given as follows:

$$H(0)_{\mathrm{DC}} = \frac{(m+1)}{2\pi d^2} \cos(\phi)^{m-1} A(\psi)_{\mathrm{eff}} \tag{2}$$

Where m is the Lambertian emission order of the emitted light beam, d is the distance between the transmitter and the receiver, ϕ and ψ are the transmitter emission angle and receiver AoI respectively, and $A(\psi)_{\mathrm{eff}}$ is the effective active area of the receiver. It is possible to define the Lambertian emission order:

$$m = -\frac{\ln 2}{\ln \cos \phi_{1/2}} \tag{3}$$

Where $\phi_{1/2}$ is the half emission angle of the transmitter. The receiver effective area can be defined as:

$$A(\psi)_{\mathrm{eff}} = A_{\mathrm{det}} G_{\mathrm{OC}} \cos(\psi) \mathrm{rect}(\psi) \tag{4}$$

In this case, A_{det} is the detector area, G_{OC} is the gain of an optical concentrator and $\mathrm{rect}(\psi)$ is a rectangular function that allows to factor the effect of its Field of View (FOV). It is defined as:

$$\mathrm{rect}(\psi) = \begin{cases} 1 & \text{if } \psi \leq \psi_{\mathrm{FOV}} \\ 0 & \text{in all other cases} \end{cases} \tag{5}$$

Where ψ_{FOV} is the concentrator FOV. At this point, it is possible to write the equation that allows the amount of optical power that hits the external layer of the optical filter put in front of the receiver, $P_{\mathrm{rx}}^{\mathrm{opt}}$, to be calculated:

$$P_{\mathrm{rx}}^{\mathrm{opt}} = P_{\mathrm{tx}}^{\mathrm{opt}} H(0)_{\mathrm{DC}} \tag{6}$$

Where $P_{\mathrm{tx}}^{\mathrm{opt}}$ is the optical power coming from the transmitter, and $H(0)_{\mathrm{DC}}$ is the optical path loss, calculated in Equation 2. From here, in order to calculate the electrical power generated after the receiver, it is possible to write:

$$P_{\mathrm{rx}}^{\mathrm{elec}} = (P_{\mathrm{rx}}^{\mathrm{opt}} \int_{\alpha}^{\beta} S_{\mathrm{tx}}(\lambda) T_{\mathrm{OF}}(\lambda) R(\lambda) \mathrm{d}\lambda)^2 \tag{7}$$

Moreover, $S_{\mathrm{tx}}(\lambda)$ is the transmitter emission spectrum, $T_{\mathrm{OF}}(\lambda)$ is the transmission characteristic of the optical filter before the receiver, while $R(\lambda)$ is the responsivity of the receiver. α and β are the upper and lower limit of the considered wavelength range, which are $\alpha = 400$ nm and $\beta = 700$ nm in this paper. It also has to be noted that each receiver is simultaneously hit by the light beams coming from every TE in range, and this results in an interference component in the generated electrical signal. If $P_{\mathrm{sig}}^{\mathrm{elec}}$ is the electrical power generated by the signal component and $P_{\mathrm{int}}^{\mathrm{elec}}$ the one generated from the interference, it is possible to write the expression of the electrical SINR for the receiver:

$$\gamma = \frac{P_{\mathrm{sig}}^{\mathrm{elec}}}{\sigma_{\mathrm{n}}^2 + P_{\mathrm{int}}^{\mathrm{elec}}} \tag{8}$$

Where σ_{n}^2 is the noise power spectral density of the system.

Table 1: LEDs and optical filters spectral parameters.

	Central Wavelength [nm]		FWHM [nm]	
	LED	Filter	LED	Filter
Blue	460	452	26	45
Green	523	525	35	50
Amber	590	590	21	20
Red	623	632	19	22

Table 2: Simulation parameters.

Parameter	Numeric Value
LEDs peak emitted power	0.69 W
Concentrator gain	3.5
Concentrator FOV	120 deg
Single receiver area	8 mm^2
Modulation bandwidth	40 MHz

3.2 Simulations

Tables 1 and 2 summarise the LEDs and optical filters' characteristics, and the simulation parameters, respectively. Three simulations have been set up and conducted by means of custom code. In all these, a room with length, width and height of respectively 10 m, 10 m, and 3 m is considered. The ceiling hosts 25 densely deployed LiFi APs, each made up by an array of 4 individually addressable LEDs. The resulting network is thus made up of 100 TEs, and each user can be assigned to one of them. The room is then populated with 4 users whose mobility behaviour and use of Classic or Adaptive WDMA depend on the simulation phase. The considered modulation scheme is On-Off Keying (OOK). Each simulation will now be described in detail.

3.2.1 Simulation 1. The first simulation investigates the impact of the PS phenomenon. A total of 4 users, with their devices' receivers always pointing upwards and using the Classic WDMA scheme, sweep every available position in the room. Then, they provide an estimation of the average Achievable Data Rate (ADR), a figure showing the spatial distribution of the ADR, and the Connection Loss (CL) rate. The CL is defined here as the probability of achieving SINR less than -6 dB. This simulation is repeated twice: the first time the effects of the PS phenomenon are included, while in the second they are taken out of the computation. This will help to understand the impact of this phenomenon.

3.2.2 Simulation 2. The second simulation is similar to Simulation 1, the only difference being that the employed scheme is the Adaptive WDMA. This will only be repeated once, while including the PS phenomenon, with the objective of showing how the Adaptive WDMA scheme can contrast such undesired effect.

3.2.3 Simulation 3. Simulation 3 is designed to show the performance gain of the Adaptive WDMA in an everyday use scenario. It consists of 10.000 iterations, and in each iteration, every user is assigned a random position and orientation. The position within the room is described by the x and y coordinates, while the orientation is described by the two angles, azimuth and elevation. The position and the azimuth angle follow a uniform distribution. The elevation angle follows a Gaussian distribution, with a mean of 30° and a standard deviation of 8.9°, as in [12] for walking activities. The simulation is repeated two times, the first while employing the Classic WDMA scheme, while Adaptive WDMA is used in the second. For each simulation repetition and each user, the Cumulative Density Function (CDF) of the ADR, the average ADR across all users, and the CL rate will be evaluated. These are averaged over 10.000 iterations.

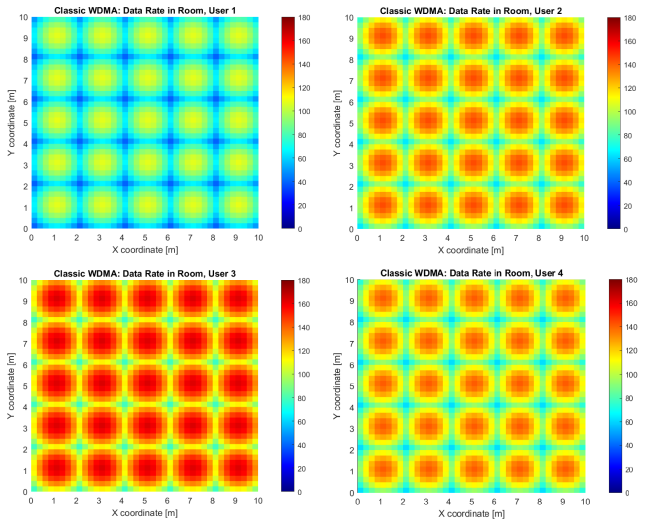

Figure 2: Achievable data rate distribution in a 10x10x3 m room for 4 users employing Classic WDMA without the contribution of the PS phenomenon. The assigned channel is fixed for each user.

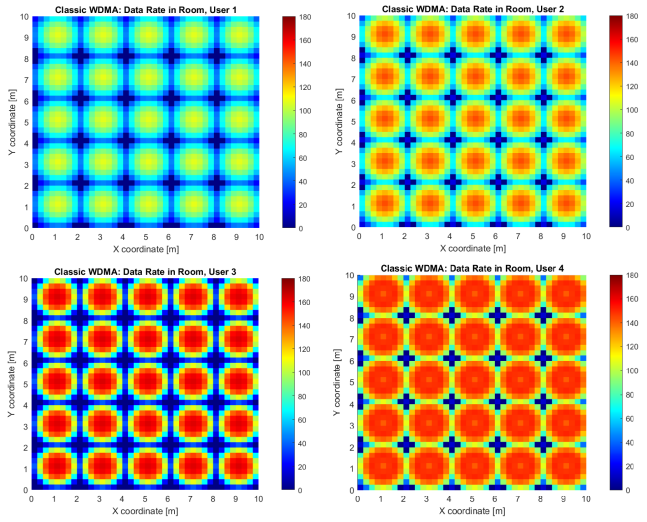

Figure 3: Achievable data rate distribution in a 10x10x3 m room for 4 users employing Classic WDMA including the contribution of the PS. The assigned channel is fixed for each user.

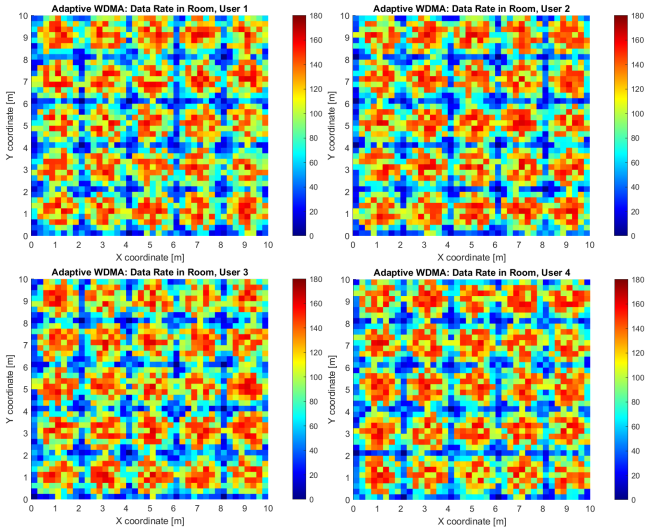

Figure 4: Achievable data rate distribution in a 10x10x3 m room for 4 users employing Adaptive WDMA including the contribution of the PS phenomenon. The assigned channel is determined for each user by maximising the aggregate SINR.

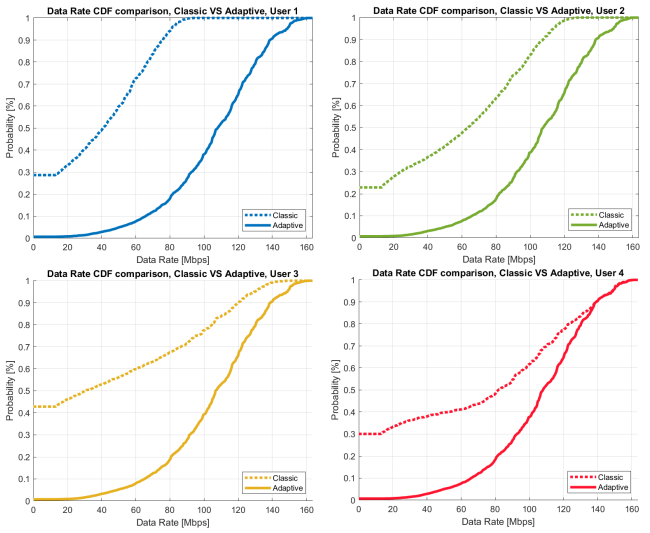

Figure 5: CDF of data rate comparison for 4 users employing Classic VS Adaptive WDMA. Each CDF is obtained over 10.000 iterations in which each user has a random position and orientation.

4 RESULTS

In this section, the simulation results will be reported and discussed. These are also summarised in Tables 3-5.

As it can be seen by comparing Figures 2-3, the PS phenomenon introduces a detriment to the performances. In fact, when this aspect is not taken into account, the ADR goes from 77.7 to 128.0 Mbps, depending on the user, and the average is 105.82 Mbps across all 4 users. The performance spread of the users can be explained with the different overlaps in the emission and transmission spectra of coupled LEDs and optical filters, and they relate to this particular aspect in the design of the front-end. In these conditions, the users experience no CL. When the simulation is repeated while including the PS, it can be seen from Figure 3 that the network's performances suffer a degradation. In fact, the ADR now ranges from 67.9 to 124.3 Mbps, and the average across all users is 95.47 Mbps. The CL rate figure in this case ranges from 5.7 to 9.3 %, meaning that even when the receivers are pointing upwards, the PS is causing outages. The average CL rate across all users is 7.12 % in this case. It has to be stressed that in these two figures, the remarkable differences in the individual users' performances, are due to how the front-end is designed. More specifically, they are dependent on how well the LEDs' emission spectra and the optical filters' transmission spectra overlap.

Figure 4 shows the results of Simulation 2. In this setting, the ADR ranges from 90.4 to 92.4 Mbps and the average is 91.62 Mbps. The CL rate ranges from 0.4 to 0.6 %, with an average of 0.52 %. It can be seen that the Adaptive WDMA is able to reduce the CL considerably with respect to the Classic scheme. This is because of the added flexibility in the choice of the RE, that gives UEs the option of using the one that is more favourable, regardless of their assigned TE. This reduces the CL figure by enabling more connections to be established, even if in these cases the resulting speed is lower than the average and contributes towards sensibly lowering the ADR figure.

As the combined effects of random position and orientation and PS are taken into account in Simulation 3, the Classic WDMA scheme suffers a considerable performance loss. On the contrary, the Adaptive WDMA scheme shows its full potential, achieving a significant improvement. Figure 5 shows the CDF of the Data Rate for each of the 4 users in the conditions described in subsection 3.2.3, when the Classic WDMA scheme is employed. In this situation, the ADRs (averaged for each user over the 10.000 iterations) range between 53.0 and 98.0 Mbps and the CL rate is between 23 and 43 %. The average across all users is 76.7 Mbps, and the average CL rate is 31.25 %. If the simulation is repeated while using the Adaptive WDMA scheme (users' CDFs shown in Figure 5), there is a substantial improvement in the performances. Notably, the ADR has a very tight range in this setting, between 105 and 106 Mbps, with an average of 105.7 Mbps. The CL rate is also much lower, ranging from 0.7 to 0.8 % with an average of 0.72 %.

By comparing these figures, one can realise that the advantages of Adaptive WDMA in this use case are twofold: the users are served better, and with higher fairness.

5 CONCLUSIONS

In this paper a novel WDMA channel allocation scheme has been presented, based on exploiting the channel separation offered by the combined effects of the PS phenomenon and random orientation. In fact, simulation results demonstrate that this is a limitation, preventing the network to establish a reliable communication when using a fixed channel allocation scheme (such as a state-of-the-art Classic WDMA).

Table 3: Results for Simulation 1. The Passband Shift phenomenon has the effect of decreasing both the number of reliable connections established, and the Average Data Rate when a connection occurs.

	User 1	User 2	User 3	User 4	Average
Average Data Rate, with PS	67.9 Mbps	94.9 Mbps	94.8 Mbps	124.3 Mbps	95.47 Mbps
Connection Loss, with PS	7.8 %	5.7 %	9.3 %	5.7 %	7.12 %
Average Data Rate, no PS	77.7 Mbps	110.1 Mbps	128.0 Mbps	107.5 Mbps	105.82 Mbps
Connection Loss, no PS	0.0 %	0.0 %	0.0 %	0.0 %	0.0 %

Table 4: Results for Simulation 2. When all UEs' receivers point upwards, the Adaptive WDMA scheme offers a more reliable connection.

	User 1	User 2	User 3	User 4	Average
Average Data Rate, with PS	90.4 Mbps	92.4 Mbps	91.5 Mbps	92.2 Mbps	91.62 Mbps
Connection Loss, with PS	0.6 %	0.5 %	0.6 %	0.4 %	0.52 %

Table 5: Results for Simulation 3. The Adaptive WDMA scheme brings a significant improvement for the system's performances when the combined effects of PS and random position and orientation are taken into account.

	User 1	User 2	User 3	User 4	Average
Average Data Rate, Classic	53.0 Mbps	73.0 Mbps	83.0 Mbps	98.0 Mbps	76.75 Mbps
Connection Loss, Classic	29.0 %	23.0 %	43.0 %	30.0 %	31.25 %
Average Data Rate, Adaptive	106.0 Mbps	106.0 Mbps	105.0 Mbps	106.0 Mbps	105.75 Mbps
Connection Loss, Adaptive	0.7 %	0.7 %	0.8 %	0.7 %	0.72 %

Adaptive WDMA can contrast this effect, by adaptively selecting the best TE-RE combination that maximises the aggregate SINR. In fact, simulation results show that when the random position and orientation of the users is taken into account, the Adaptive WDMA scheme is able to improve the ADR, serve users with better fairness, and reduce connection losses to 0.7-0.8 % while the Classic WDMA only achieves 23-43 %, depending on the channel employed and the front-end design choices of LEDs and optical filters' spectral characteristics.

On the other hand, results show that if the orientation is fixed and pointing upwards, the improvement over the Classic WDMA scheme is smaller. In fact, if the users share the same position and orientation at all times, the system can only reap the benefits of the added flexibility in choosing the RE. The TE-user assignation does not matter in this situation, as without separation in position and orientation between the UEs, there is no benefit in preferring one particular pairing over another.

ACKNOWLEDGMENTS

This work has been funded by the European Union's Horizon 2020 research and innovation programme under the Marie Skłodowska Curie grant agreement ENLIGHT'EM No. 814215.

REFERENCES

[1] Mohamed Amine Arfaoui, Mohammad Dehghani Soltani, Iman Tavakkolnia, Ali Ghrayeb, Chadi M. Assi, Majid Safari, and Harald Haas. 2021. Measurements-Based Channel Models for Indoor LiFi Systems. *IEEE Transactions on Wireless Communications* 20, 2 (2021), 827–842. https://doi.org/10.1109/TWC.2020.3028456

[2] John R. Barry and Joseph M. Kahn. 1995. Link design for nondirected wireless infrared communications. *Appl. Opt.* 34, 19 (Jul 1995), 3764–3776. https://doi.org/10.1364/AO.34.003764

[3] Jiaxuan Chen, Iman Tavakkolnia, Cheng Chen, Zhaocheng Wang, and Harald Haas. 2020. The Movement-Rotation (MR) Correlation Function and Coherence Distance of VLC Channels. *Journal of Lightwave Technology* 38, 24 (2020), 6759–6770. https://doi.org/10.1109/JLT.2020.3018884

[4] Mohammad Dehghani Soltani, Ardimas Andi Purwita, Iman Tavakkolnia, Harald Haas, and Majid Safari. 2019. Impact of Device Orientation on Error Performance of LiFi Systems. *IEEE Access* 7 (2019), 41690–41701. https://doi.org/10.1109/ACCESS.2019.2907463

[5] Mohammad Dehghani Soltani, Ardimas Andi Purwita, Zhihong Zeng, Cheng Chen, Harald Haas, and Majid Safari. 2020. An Orientation-Based Random Waypoint Model for User Mobility in Wireless Networks. (2020), 1–6. https://doi.org/10.1109/ICCWorkshops49005.2020.9145333

[6] Ilker Demirkol, Daniel Camps-Mur, Josep Paradells, Marc Combalia, Wasiu Popoola, and Harald Haas. 2019. Powering the Internet of Things through Light Communication. *IEEE Communications Magazine* 57, 6 (2019), 107–113. https://doi.org/10.1109/MCOM.2019.1800429

[7] Pengfei Ge, Xiao Liang, Jiaheng Wang, Chunming Zhao, Xiqi Gao, and Zhi Ding. 2019. Optical Filter Designs for Multi-Color Visible Light Communication. *IEEE Transactions on Communications* 67, 3 (2019), 2173–2187. https://doi.org/10.1109/TCOMM.2018.2883422

[8] Pengfei Ge, Xintong Ling, Jiaheng Wang, Xiao Liang, Shuo Li, and Chunming Zhao. 2021. Optical Filter Bank Modeling and Design for Multi-Color Visible Light Communications. *IEEE Photonics Journal* 13, 1 (2021), 1–19. https://doi.org/10.1109/JPHOT.2021.3053177

[9] Pengfei Ge, Xintong Ling, Jiaheng Wang, Xiao Liang, Rong Zhang, and Chunming Zhao. 2019. Optical Filter Bank for Multi-Color Visible Light Communications. In *2019 IEEE Global Communications Conference (GLOBECOM)*. 1–6. https://doi.org/10.1109/GLOBECOM38437.2019.9013914

[10] Harald Haas and Cheng Chen. 2015. What is LiFi?. In *2015 European Conference on Optical Communication (ECOC)*. 1–3. https://doi.org/10.1109/ECOC.2015.7341879

[11] J.M. Kahn and J.R. Barry. 1997. Wireless infrared communications. *Proc. IEEE* 85, 2 (1997), 265–298. https://doi.org/10.1109/5.554222

[12] Mohammad Dehghani Soltani, Ardimas Andi Purwita, Zhihong Zeng, Harald Haas, and Majid Safari. 2019. Modeling the Random Orientation of Mobile Devices: Measurement, Analysis and LiFi Use Case. *IEEE Transactions on Communications* 67, 3 (2019), 2157–2172. https://doi.org/10.1109/TCOMM.2018.2882213

[13] Shivani Rajendra Teli, Stanislav Zvanovec, and Zabih Ghassemlooy. 2018. Optical Internet of Things within 5G: Applications and Challenges. In *2018 IEEE International Conference on Internet of Things and Intelligence System (IOTAIS)*. 40–45. https://doi.org/10.1109/IOTAIS.2018.8600894